Preparation and Characterization of Side-Chain Liquid-Crystalline Polyoxetanes Anchoring a Pendant Spacer-Separated Mesogen at the Tertiary-Like C-3 Carbon of the Oxetane Unit

Hiroshi Ogawa, Yasutake Kodera, Shigeyoshi Kanoh, Akihiko Ueyama,† and Masatoshi Motoi*

Department of Chemistry and Chemical Engineering, Faculty of Engineering, Kanazawa University, 2-40-20 Kodatsuno, Kanazawa 920

†New Materials Development Department, Industrial Technology Center of Fukui Prefecture, 61 Kawaiwashizuka, Fukui 910

(Received August 11, 1997)

Polyoxetanes anchoring a pendant spacer-separated mesogen at the tertiary-like C-3 carbon of the oxetane unit were prepared by cationic ring-opening polymerization of the corresponding oxetane derivatives. The resulting polymers were liquid-crystalline substances showing textures assignable to the nematic or smectic mesophase over a wide temperature range from about 260 °C to room temperature. These mesogens also behaved in the manner similar to that of the mesogens in the analogous polyoxetanes attached by a methyl side chain at the quaternary C-3 carbon, although the less bulky polymer backbone in the present work indicated a somewhat higher isotropic phase-transition temperature than that of the methyl-substituted analogs. In both types of the polyoxetanes, their mesophase patterns were influenced by the core structure and alkoxy tail length in the pendant mesogen, but not by the bulkiness of the second side chains, H and CH_3, attached at the C-3 carbon of the polyoxetane unit.

Our investigation of applying polyoxetanes to the supporting matrices of functional polymers has been continued. In one of the applications, we found polyoxetanes that are promising as the main chain of side-chain liquid-crystalline polymers anchoring pendant spacer-separated mesogens, the core of which contained both of benzoate and azobenzene moieties,[1,2] although other cores, such as biphenyl, phenyl cyclohexanecarboxylate, and trisbenzoate moieties, were also useful as pendant mesogens of polyoxetanes.[3—6] Here, we are interested in knowing what influence is exerted on the liquid-crystalline properties of these polyoxetanes by the structures of their main chains and pendant mesogens, since these findings will provide information about synthesizing the desired liquid-crystalline polymers with thermal stability and functioning ability. In our previous studies, in order to know the role of the benzoate and azobenzene moieties and the tail in forming mesophases, the polymers of oxetanes, **2a**, **2c-*n***, and **2d-*n***, were prepared with an ether–boron trifluoride (1/1) complex ($Et_2O{\cdot}BF_3$) as an initiator in dichloromethane (DCM) at room temperature of 15—25 °C (Scheme 1). The liquid-crystalline properties of the polymers thus obtained were examined by differential scanning calorimetry (DSC) and polarized optical micrography (POM). These results revealed that the benzoate as well as the azobenzene can be regarded as being one of the important segments in the mesogen core of thermally stable liquid-crystalline polyoxetanes. Thus, the influence of the mesogen structure on the liquid-crystalline properties was investigated for polyoxetanes having a pendant mesogen in one side chain at the quaternary C-3 carbon of the oxetane unit. However, there is little information concerning such an influence exerted by unmesogenic substituents in the other side chain at the C-3 position, which we henceforth call the second side chain, although the preparation and characterization of liquid-crystalline polyoxetanes having siloxane-containing substituents or alkoxymethyl substituents as the second side chain were reported recently.[4,7] In this paper we describe the preparation and characterization of polymers derived from oxetanes, **1a**, **1b**, **1c-*n***, **1d**, and ***m*-1d**, having no second side chain, and exhibit the influence of the second side chain on the structure and thermal stability of a mesophase compared with the results obtained for analogs having the second side chain of methyl.

Results and Discussion

Preparation of Oxetanes and Their Polymers. Oxetane monomers used in this study were prepared through synthetic routes shown in Scheme 2. 3-Oxetanol (**3**) was obtained as a crude product according to a modified procedure of a method reported by Baum and co-workers;[8] although they protected the hydroxy group of a chlorohydrin derivative with ethyl vinyl ether, we used 2,3-dihydro-4*H*-pyran as a protecting agent. *p*-Toluenesulfonate **5** was obtained as a pure product by a reaction of crude **3** with *p*-toluenesulfonyl chloride in a 10% aqueous NaOH solution, followed by recrystallization; however, it was difficult or troublesome to isolate **3** by ordinary techniques, e.g., fractional distillation and column chromatography. Moreover, an attempt in ob-

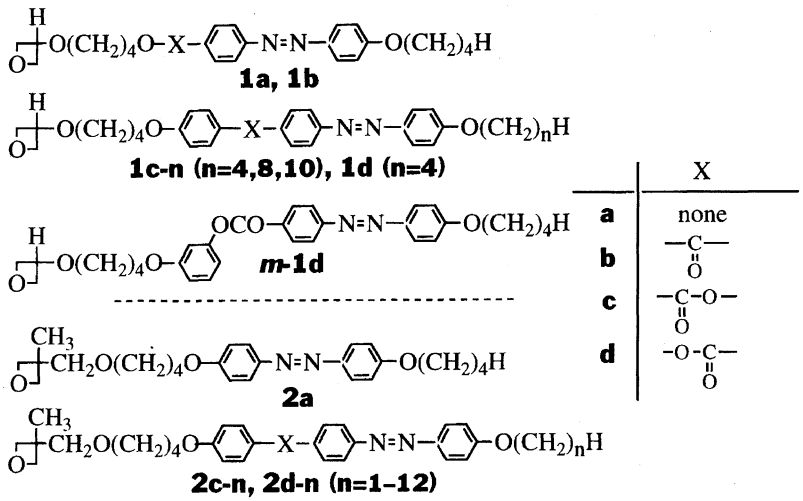

Scheme 1. Oxetane monomers used in this study.

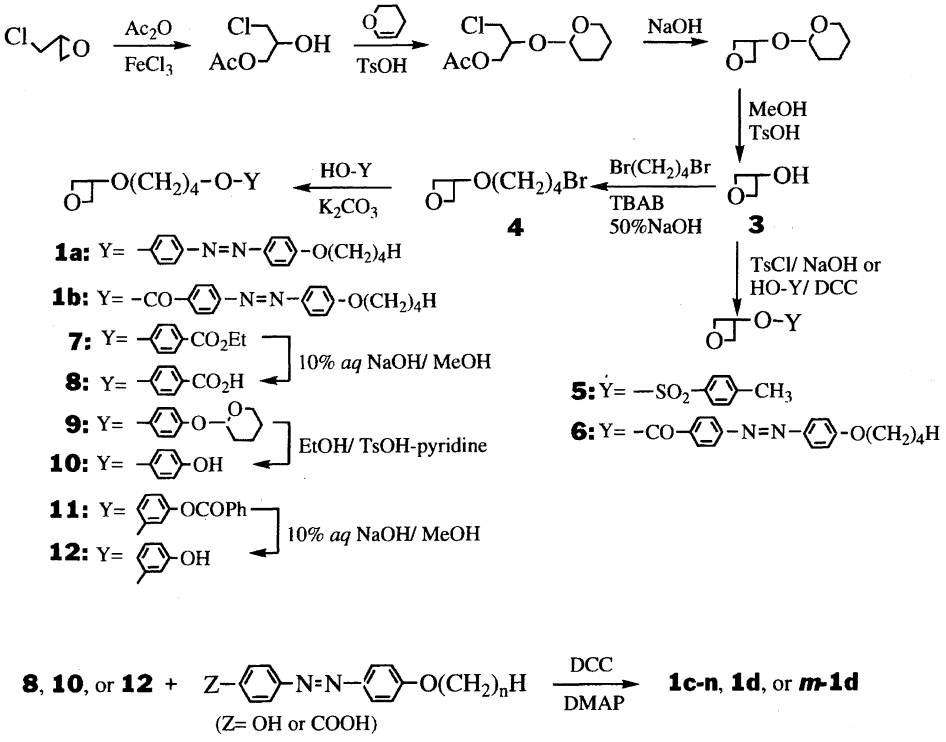

Scheme 2. A synthetic route of oxetanes, **1a**, **1b**, **1c-*n***, **1d**, and ***m*-1d**, and their polymers.

taining pure **3** through alkaline hydrolysis of purified **5** also failed; the sulfonate **5** was quite unsusceptible to the alkaline hydrolysis. Pure bromide **4** was smoothly obtained by a reaction of the crude alcohol **3** with a 3-fold molar amount of 1,4-dibromobutane under phase-transfer catalytic conditions using tetrabutylammonium bromide (TBAB) in 50% aqueous NaOH at reflux temperature, followed by distillation of the reaction mixture. The terminal bromo group of **4** was converted to the desired mesogen structures through the corresponding reaction steps. After recrystallization from an appropriate solvent, these monomers were also subjected to cationic ring-opening polymerization with a 0.08 molar amount of $Et_2O{\cdot}BF_3$ to the monomer in DCM at room temperature of 15—25 °C. The polymerization solution was poured into methanol to precipitate the polymer product separated from the unchanged monomer. The results of the polymerization are summarized in Table 1. In each the polymerization product, an oligomer fraction with gel permeation chromatography (GPC)-average molecular weight (M_{gpc}) below 3000 was contained in 6—20% of the total area in the GPC curve. The production of the oligomers is not ascribed to the existence of the long side-chain or its polar functional groups in the oxetane monomer, since it is generally known that oxetanes have a strong tendency to produce a cyclic tetramer as a main ingredient in the oligomer fraction, as shown in the cationic ring-opening polymerization of oxetane and its 3,3-dimethyl and 3,3-diethyl analogs.[9—11] Oxetane **6**, linking a mesogenic side-chain through no spacer,

Table 1. Preparation of Polyoxetanes by Ring-Opening Polymerization with $Et_2O{\cdot}BF_3$[a]

Monomer	$[M]_0^{c)}$	Polymer product[b]		
		Yield	$10^{-3} \times M_{gpc}$	Oligomer[d]
	mol dm^{-3}	%		%
5	2.20	86	10.4	27
1a	1.00	73	30.6	26
1b	0.94	70	40.2	7
1c-4	0.77	85	22.5, 12.6[e]	10
1c-8	0.52	83	6.3[f]	14
1c-10	0.50	92	7.2[f]	13
1d	0.58	77	3.6[f]	38
6	0.57	64	10.4	>90
***m*-1d**	0.58	98	21.5, 12.5[e]	10

a) Carried out with 0.08 molar equiv of $Et_2O{\cdot}BF_3$ to monomer in DCM at rt for 50 h. b) Obtained by reprecipitation from DCM to methanol. c) An initial monomer concentration. d) Content of an oligomer fraction with molecular weight below 3000 was estimated from an area ratio in a GPC curve. e) Two peak tops were observed in a GPC curve. f) For a soluble part in THF (GPC eluent).

gave a considerable amount of oligomers under the same polymerization conditions, although polymers lying in a M_{gpc} region of 7000 to 40000 were contained in a minor fraction (below 10% of the total area) by GPC. In **6**, the acyloxy group directly linked to the C-3 carbon of the oxetane ring may tend to interfere with propagation in the ordinary ring-opening polymerization mechanism, since the acyloxy and phthalimide groups linked to the C-3 carbon of the oxetane ring through only a methylene linkage interfered with the ordinary propagation of the oxetane ring in the presence of $Et_2O{\cdot}BF_3$, i.e., the carbonyl oxygen atoms of the acyloxy and phthalimido groups nucleophilically attacked the C-2 carbon of the oxetane ring to give 2,6,7-trioxa- and 2,6,7-dioxazabicyclo[2.2.2]octane structures, respectively.[12,13] On the other hand, the sulfonyl oxygen of the corresponding sulfonate did not act as an active species in the participation of neighboring groups.[13] In this study, oxetane **5** having a pendant sulfonate group through no spacer also behaved in the ordinary ring-opening polymerization mechanism to give the corresponding polyoxetane with a M_{gpc} of 10400. Poly(**1c-8**), poly(**1c-10**), and poly(**1d**) were not completely soluble in the THF used as an eluting medium of GPC, although they were soluble in DCM and chloroform; thus, the M_{gpc} region of 4000 to 6000 was estimated by only GPC for their THF-soluble parts. These results may be based on the reason that the THF-insoluble parts have a considerably high molecular weight and/or a highly regulated tacticity.

The ^{1}H NMR spectra of poly(**1b**) and its monomer (**1b**) are shown in Fig. 1. The protons (H^a to H^m) of **1b** are easily assigned to the corresponding signals ((a) to (m)). This spectrum resembles that of poly(**1b**), except for the chemical shift values and patterns of the methine and methylene protons (H^i and H^h) in the main chain; these signals resonate at δ = 4.5—5.0 and 3.6—3.3, respectively, before and after ring-opening. Such a shifting of signals to a higher magnetic field after ring-opening was also observed for the polymerization of **2a**, **2c-*n***, and **2d-*n***. These findings are interpreted on the basis of the fact that the methine (or methyl) and methylene protons in and adjacent to the oxetane ring are linked through sp^2-like σ bonds.[14] A change in the linking pattern from the oxetane ring to the polyether chain was also confirmed by the IR spectra of the monomer and its polymer. The polymer indicated an IR band due to a polyether linkage at 1100 cm^{-1} in place of an IR band at 980 cm^{-1} due to a cyclic ether linkage in the monomer. Similarly, the IR

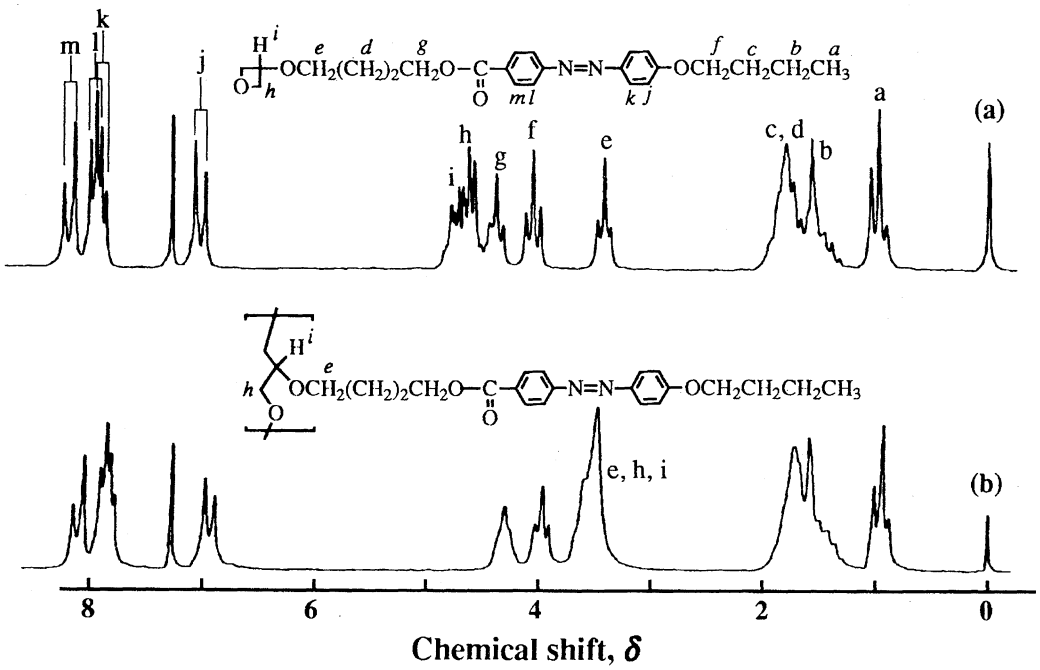

Fig. 1. ^{1}H NMR spectra of (a) oxetane, **1b**, and (b) its polymer, poly(**b**).

and ^{1}H NMR spectra characteristic of the oxetane and polyoxetane structures were also observed for the other oxetane monomers and their polymers used in this study. Furthermore, these data of elemental analysis approximately agreed with the theoretical values, as shown in Table 2, except for the ring-opened product from **6**.

Liquid-Crystalline Property of Oxetane Monomers. The DSC curves of oxetanes, **1a**, **1b**, **1c-*n***, **1d**, and ***m*-1d** are shown in Figs. 2 and 3 on second heating and first cooling scans, respectively. DSC curves on first heating scan are also exemplified in Fig. 2 for **1a**, **1b**, **1c-10**, and ***m*-1d**, which indicated DSC curves different from those on the second heating scan. Liquid-crystalline mesophases (nematic or smectic) were identified, although roughly, based on texture patterns observed in a POM measurement. Since the POM sample was prepared by melting the virgin sample on a cover glass with degassing, however, it was difficult to identify the mesophases of virgin samples on a first heating scan. By comparing DSC curves between **1a** and **1b** and between **1b** and **6**, it is indicated that the mesomorphic temperature range is not improved by the existence of an ester carbonyl or a tetramethylene spacer between the oxetane ring and the azobenzene moieties; these monomers gave crystalline phases rather than liquid-crystalline phases. However, the spacer-linked 1,4-phenylene segments in **1c-*n*** and **1d** had an remarkable effect on expanding the mesomorphic temperature range and raising the isotropic phase transition temperature (T_i), while the 1,3-phenylene of ***m*-1d** hardly had such an effect. Nevertheless, the oxetanes, having the 1,4- and 1,3-phenylene segments in the mesogen, tended to form a nematic mesophase.

In a comparison between DSC curves upon second heating and first cooling for each of **6**, **1a**, and ***m*-1d**, it is considered that these monomers behaved in the manner of a monotropic phase transition, since the transition from isotropic to nematic or smectic phases was observed by DSC and POM only during the cooling process. Monomer **1b** also showed the monotropic nematic mesophase. When **1b** was cooled from an isotropic phase upon a POM measurement, a texture due to the nematic mesophase was observed to room temperature; this texture then changed to that due to the crystalline phase after leaving the **1b** cooled at this temperature for a while. In Fig. 1c, an endothermic peak with a small enthalpy at 57 °C upon second heating may be ascribed to the nematic—isotopic phase transition of the nematic phase, which was left unchanged in parts during the nematic—crystalline phase transition upon the first cooling. Furthermore, DSC curves on the first heating seem to be unimportant, since a virgin

Table 2. Elemental Analysis Data of Polyoxetanes Used in the Present Study

Monomers and polymers	Contents of C, H, and N/%					
	Calcd			Found		
	C	H	N	C	H	N
1a	69.32	7.59	7.03	69.03	7.78	6.94
poly(**1a**)				69.31	7.55	7.03
1b	67.63	7.09	6.57	67.40	7.01	6.63
poly(**1b**)				67.53	7.15	6.29
1c-4	69.48	6.61	5.40	69.26	6.61	5.46
poly(**1c-4**)				69.18	6.61	5.19
1c-8	71.06	7.37	4.87	70.55	7.58	4.98
poly(**1c-8**)				70.80	7.29	4.87
1c-10	71.73	7.69	4.65	71.48	7.55	4.47
poly(**1c-10**)				71.47	7.80	4.56
1d	69.48	6.61	5.40	69.21	6.48	5.28
poly(**1d**)				69.21	6.59	5.36
6	67.78	6.26	7.90	67.53	6.15	7.99
poly(**6**)				66.79	6.30	7.93
***m*-1d**	69.48	6.61	5.40	69.42	6.62	5.59
poly(***m*-1d**)				69.44	6.56	5.13

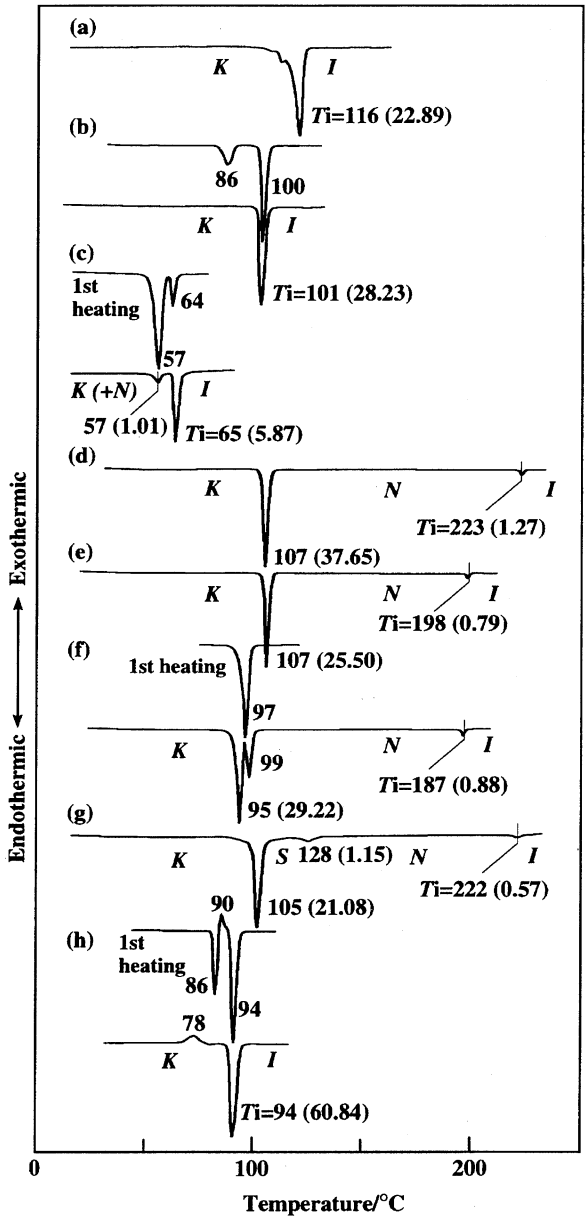

Fig. 2. DSC curves of (a) **6**, (b) **1a**, (c) **1b**, (d) **1c-4**, (e) **1c-8**, (f) **1c-10**, (g) **1d**, and (h) ***m*-1d** on 2nd heating scan. *I*,*N*,*S*, and *K* refer to isotropic, nematic, smectic, and crystalline phases, respectively. Figures in parentheses indicate enthalpy in J g^{-1}.

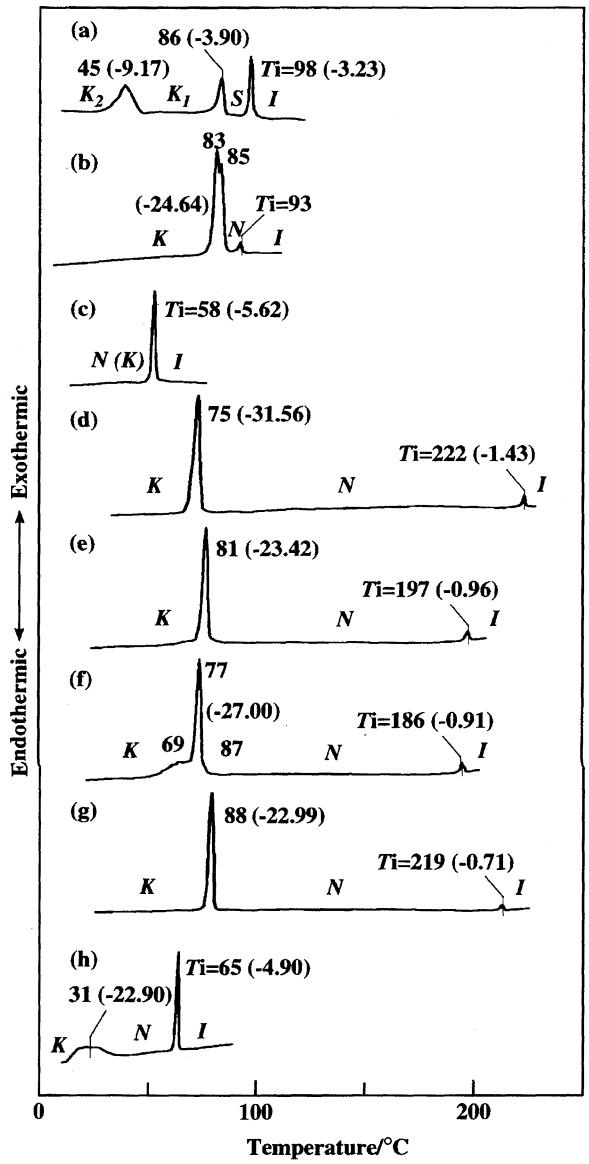

Fig. 3. DSC curves of (a) **6**, (b) **1a**, (c) **1b**, (d) **1c-4**, (e) **1c-8**, (f) **1c-10**, (g) **1d**, and (h) ***m*-1d** on 1st cooling scan. See Fig. 2 for notes.

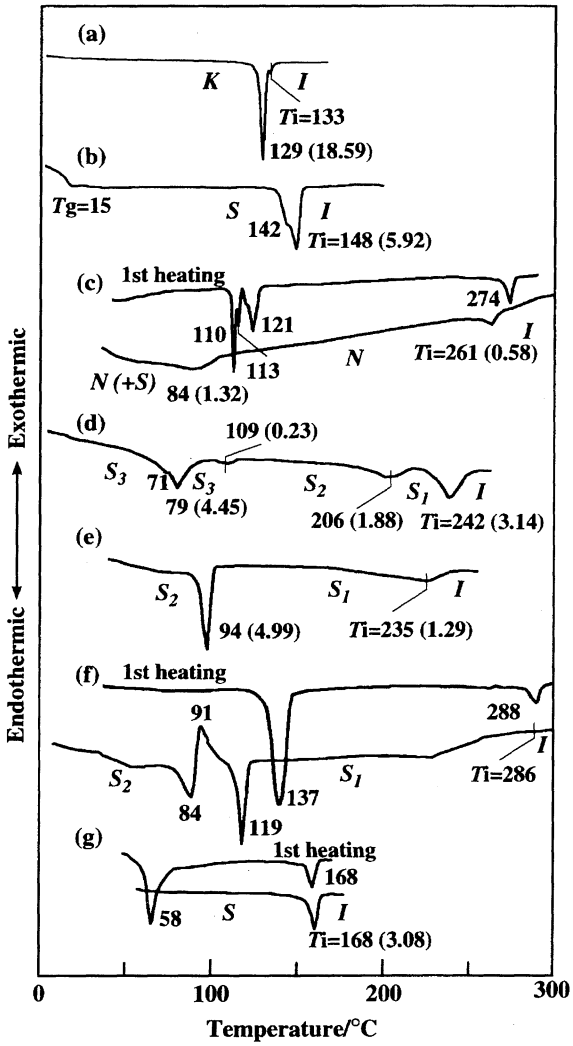

Fig. 4. DSC curves of (a) poly(**1a**), (b) poly(**1b**), (c) poly(**1c-4**), (d) poly(**1c-8**), (e) poly(**1c-10**), (f) poly(**1d**), and (g) poly(***m*-1d**) on 2nd heating scan. See Fig. 2 for notes.

sample tends to have a structure different from that formed after the first heating scan. Since the structure of a virgin sample, obtained by recrystallization from an appropriate solvent, is formed in the presence of solvent molecules, the mesogens of the virgin sample are not yet packed in a right matrix of a crystal or liquid-crystal. Thus, DSC curves recorded after a second heating scan resembled the DSC curve of the second heating scan, but not that of the first heating scan.

Liquid-Crystalline Property of Monoside-Chain Type Polyoxetanes. Effect of Ester Linkage: The DSC curves of polyoxetanes, poly(**1a**), poly(**1b**), poly(**1c-*n***), poly(**1d**), and poly(***m*-1d**), are shown in Figs. 4 and 5 on the second heating and first cooling scans, respectively. DSC curves on the first cooling scan are also exemplified in Fig. 4 for poly(**1c-4**), poly(**1d**), and poly(***m*-1d**). The polymer of **1a**, which has only an azobenzene in the mesogen core, showed a nematic mesophase over a narrow temperature range, although it seemed faintly wider than the mesomorphic temperature range of **1a**. However, poly(**1b**) showed a smectic mesophase, as shown by a texture of small fans [(A) in Fig. 6], in the temperature range below T_i, which was somewhat higher than the T_i of poly(**1a**), in spite of the fact that monomer **1b** showed 25—35 °C lower T_i values than did **1a**. These findings indicate that the formation of a mesophase is obviously favored by the existence of the ester carbonyl in the pendant core, i.e., immobilized to the polyoxetane main chain, the 4-(4-butoxyphenylazo)benzoyl moiety becomes suitable for constructing a highly ordered mesophase, such as the smectic structure, rather than a crystalline structure. The tendency for the pendants of poly(**1b**) to form the liquid-crystalline structure may be ascribed to a polar, plate-like structure of the 4-(4-butoxyphenylazo)benzoyl, which lies in a system widely conjugated through π-electrons from the butoxy ether to the ester carbonyl.[2] In fact, as indicated by the ^{1}H NMR spectra of **1b** and poly(**1b**) (Fig. 1), these but-

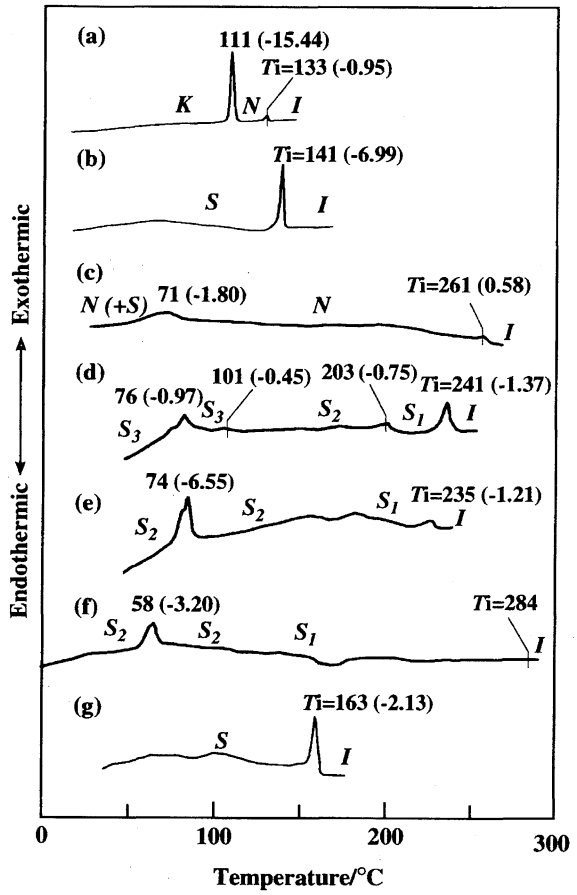

Fig. 5. DSC curves of (a) poly(**1a**), (b) poly(**1b**), (c) poly(**1c-4**), (d) poly(**1c-8**), (e) poly(**1c-10**), (f) poly(**1d**), and (g) poly(***m*-1d**) on 1st cooling scan. See Fig. 2 for notes.

oxy tails obviously have a positive mesomeric effect, since the aromatic protons ortho to the butoxy group resonate at lower chemical shifts of $\delta = 6.9$—7.1 than the chemical shift of $\delta = 7.4$—7.6 for the meta protons of unsubstituted azobenzene.

Influence of Ring Substitution Pattern in 1,3- and 1,4-Phenylenes: Poly(**1d**), which possesses an 1,4-phenylene linkage besides the core, 4-(4-butoxyphenylazo)benzoyl, of poly(**1b**), showed focal-conic fan textures in the temperature range below 286 °C upon heating and below 284 °C upon cooling, as exemplified by textures (B) and (C).

The 1,3-phenylene segment in poly(***m*-1d**) inferiors to the 1,4-phenylene segment of poly(**1d**) in giving a thermally stable mesophase, as shown in a comparison between their T_i values. The bent mesogen core of poly(***m*-1d**) has a larger excluded volume than the nearly straight mesogen core of poly(**1d**), when free rotation is possible around σ bonds of C–C and C–O linkages in an ample supply of heat energy. Since the excluded volume of the core decreases by enhancing the degree of restricted rotation with lowering of temperature, attractive interactions sufficient for the pendant mesogens to organize a mesophase become possible among the mesogens. Therefore, the mesogens of poly(***m*-1d**) are packed in the liquid-crystalline state at a lower T_i than that of poly(**1d**), as exemplified by texture (D). Thus, the T_i values of poly(**1b**), poly(**1d**), and poly(***m*-1d**) were different from each other, but their POM textures were fan-shaped patterns due to the formation of the smectic mesophases, although they were not identified in detail.

Influence of the Pattern of Ester Linkage Inserted between Aromatic Rings and of Tail Length: On the contrary, in poly(**1c-4**), which possesses an ester linkage in the inverse direction of the ester linkage of poly(**1d**), the nematic mesophase was formed over a wide temperature range from about 260 °C to room temperature, as shown by threaded textures (E and F). Although *p*-spacer-substituted benzoyl segment, $-CH_2O(CH_2)_4O-C_6H_4(CO)-$, of poly(**1c-4**) also forms an attractive dipole to assemble mesogens in the nematic mesophase, this dipole is not so sufficient as the dipole of the widely conjugated 4-(4-alkoxyphenylazo)benzoyl of poly(**1d**). Such a difference in the core structures is considered to be one of the factors which exert an influence on mesophase formation. However, the widely conjugated system in the mesogen core is not necessarily required to form a highly ordered mesophase, such as the smectic, since the pendant mesogens of poly(**1c-8**) and poly(**1c-10**) can form the smectic mesophase, as shown by fan-shaped textures (G, H, and I), although their T_i values were lowered with lengthening of the tail. Therefore, the long tails act as a segment capable of facilitating the formation of the smectic mesophase. Probably, this driving force is due to the van der Waals' force enhanced by the long alkoxy tails. On the other hand, these longer tails have a larger excluded volume than the butoxy tail, resulting in lowering the T_i value.

X-Ray diffraction patterns are indicated in Fig. 7 for the samples obtained by cooling poly(**1c-4**), poly(**1c-8**), and poly(**1d**) to room temperature on POM measurement. On the basis of the X-ray diffraction pattern of poly(**1c-4**) (Fig. 7a), its texture (E) is identified as being due to the nematic mesophase, although diffraction peaks in the small angle region of $2\theta = 4$—$8°$ may indicate the formation of a smectic mesophase in minor domains; in Fig. 6, the appearance of spots in the texture (E) may also suggest the early stage in forming a smectic mesophase. However, the layer structure due to a smectic mesophase is formed in poly(**1c-8**), as revealed by the X-ray diffractgram in Fig. 7b; also, the formation of a more highly ordered mesophase is achieved in poly(**1d**), as is distinctively shown in Fig. 7c. Thus, the results of X-ray diffraction support the identification of the above-mentioned textures.

As for the influence of the mesogen structure on the liquid-crystalline property, the polymers without the second side-chain are similar to the methyl-substituted analogs, poly(**2a**), poly(**2c-*n***)s, and poly(**2d-*n***)s, as described in the following outline. Poly(**2d-*n***)s showed fan-shaped textures in the temperature range from about 250 °C to room temperature, hardly being affected by the length of the tails, except for the methoxy tail. However, in isomeric polymers, poly(**2c-*n***)s, their tail length had an influence on the mesophase pattern, but not on maintaining the mesophases over a wide temperature range from about 250 °C to room temperature. Schlieren and/or isotropic (probably due to the homeotropic

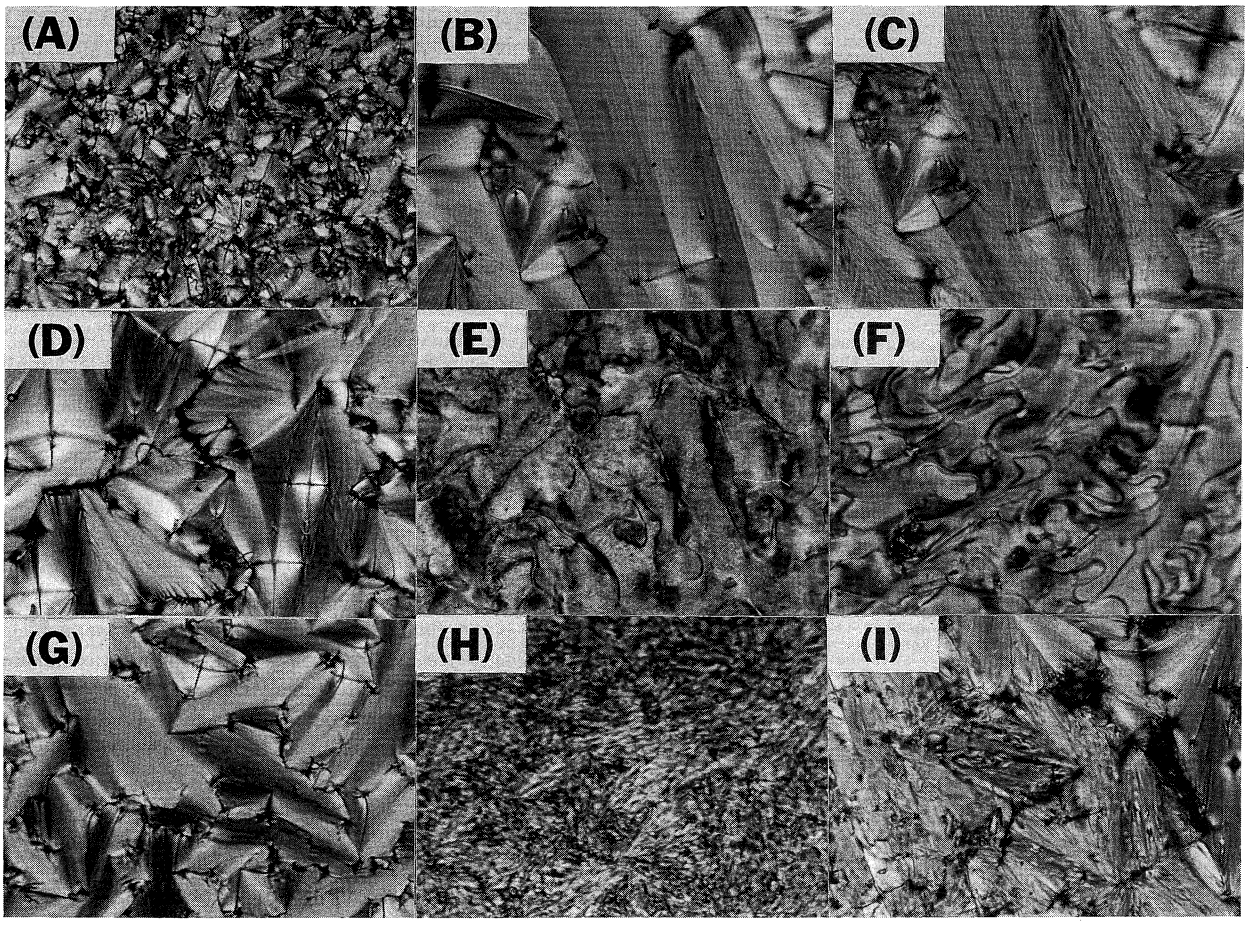

Fig. 6. POM micrographs taken at appropriate temperatures on cooling for polyoxetanes: (A) poly(**1b**), 25 °C; (B) poly(**1d**), 208 °C; (C) poly(**1d**), 24 °C; (D) poly(***m*-1d**), 23 °C; (E) poly(**1c-4**), 26 °C; (F) poly(**1c-4**), 139 °C on heating; (G) poly(**1c-8**), 198 °C; (H) poly(**1c-8**), 27 °C; and (I) poly(**1c-10**), 207 °C.

structure) textures were observed in the mesomorphic temperature range, when n was 1—3 in the tail, $O(CH_2)_nH$, and fan-shaped textures, when $n = 8$—12. When $n = 4$—7, however, schlieren and/or isotropic textures were observed in higher temperature range and a texture of meager fans in lower temperature range. Poly(**2a**), having no benzoate moiety in the mesogen core, showed a schlieren or thread-like texture in a narrow temperature range upon cooling below T_i; the texture then changed to sanded or spherulitic texture in the lower temperature range.

Influence of Second Side Chains, H and CH_3: The second side chains also affected the T_i values of polyoxetanes. For instance, the existence of a methyl side chain in poly(**2c-4**) and poly(**2d-4**) resulted in lowering the T_i value by about 10 °C, compared with those of poly(**1c-4**) and poly(**1d**) having no second side chain, suggesting that the methyl side chain behaved as a bulky segment, which interfered with an assembly of the pendant segments, until these began to be packed in the liquid-crystalline state at T_i.

The glass transition temperature (T_g) of poly(**1b**) was observed at a temperature of around 15 °C upon a heating scan (Fig. 4a). However, a distinctive change in the baseline level of the DSC curve was not noticed for most of the polyoxetanes examined in our present and previous studies.[1,2] Polyoxetanes having both the core of *p*-spacer-substituted phenyl *trans*-4-alkyl-1-cyclohexanecarboxylate and the side chain of methyl at the C-3 position of the oxetane unit were reported to have their T_g values at −0.6 to 24 °C.[5] The T_g values of several polyoxetanes with unmesogenic alkyl side chains were also determined to be in the temperature region below 0 °C, although the T_g values tended to be raised by increasing the bulkiness of the side chain, being ascribed to the intramolecular factors related to the restrictions for bond rotations.[15] In these polymers, a T_g value of −31 °C was estimated for poly(3-methyl-3-propyloxetane), which may be regarded as a model for the main chain part of liquid-crystalline polyoxetanes with the methyl side chain. We also confirmed that 3-(4-bromobutoxy)methyl-3-methyloxetane gave a viscous grease-like polymer under ring-opening polymerization conditions; probably the T_g of this polymer is below room temperature.[16] Thus, the polyoxetane main chains are considered to be fairly flexible. Therefore, when a hydrogen atom is attached at the C-3 position in place of the methyl side chain, the polyoxetane main chain can become more flexible. Furthermore, since the pendant spacers of the liquid-crystalline polymers in the present study were attached to the main chain through an ether linkage, such a structure made the main chain more flexible than the corre-

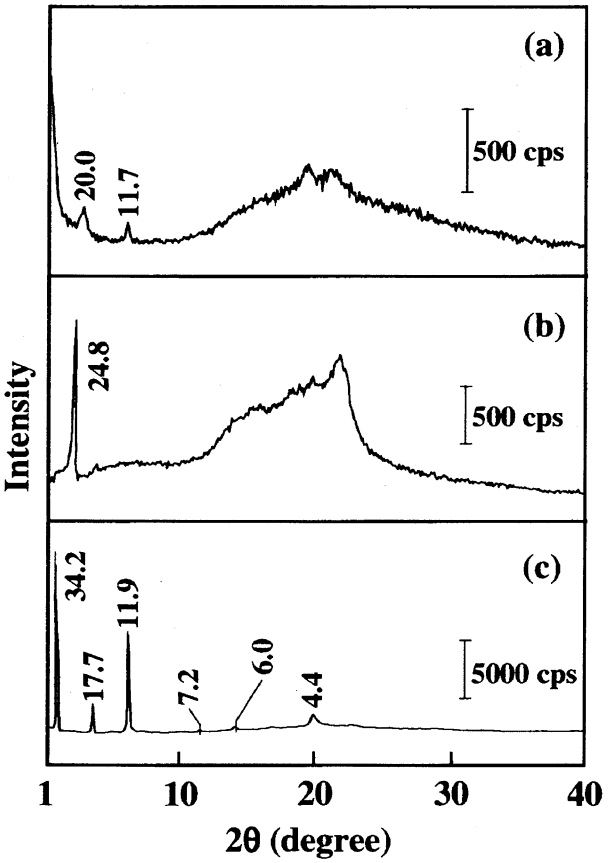

Fig. 7. X-Ray diffraction patterns of (a) poly(**1c-4**), (b) poly(**1c-8**), and (c) poly(**1d**). Figures at peak top indicate spacing in Å.

sponding polyoxetane main chain attached at the quaternary C-3 carbon by the methylene head in the pendant spacers of poly(**2c-*n***)s and poly(**2d-*n***)s. Nevertheless, these polymers showed such POM textures as the corresponding polymers without the second side chain indicated, although both types of polymers were somewhat different in their T_i values.

In addition, exo- or endothermic peaks appeared noticeably in the lower temperature range of 60 to 90 °C upon the second heating or first cooling scans. However, these are not ascribed to a phase transition of a liquid-crystalline or crystalline state, since no change in the POM texture was observed at these peak temperatures. The appearance of these peaks may be ascribable to a phase transition due to a conformational change and/or crystallization of the polymer backbone, spacer, and tail segments. It has not yet been clarified what phase transition these thermic peaks in the lower temperature range can be ascribed to.

In conclusion, novel polyoxetanes, such as poly(**1c-*n***)s and poly(**1d**), having no second side chain were liquid-crystalline substances similar to the methyl-substituted analogs, and showed the nematic or smectic mesophase over a wide temperature range from about 260 °C to room temperature. Since these mesophases seemed to be formed in domains separated from polyoxetane main chains, the mesophase patterns may hardly be influenced by the second side chains, H and CH_3, attached at the C-3 position of the oxetane unit; i.e., mesophase patterns firstly depend on the structure of a core, which coheres with each other through attractive interactions of dipoles generated in the core, and secondly on the long tail, which coheres with each other through the van der Waals' force. In addition, the formation of a highly ordered mesophase was achieved much more smoothly by immobilizing the mesogens to polymer backbones, compared with those of the corresponding monomers, suggesting that polymer backbones are one of the important structural segments in preparing liquid-crystalline polymers. It is interesting to us whether the formation of a mesophase is affected by the flexibility of a polymer backbone. This problem may be solved by comparing the liquid-crystalline property between the pendant mesogens based on the polyoxetane backbone and those based on rigider backbones, e.g., polystyrene and polymethacrylate.

Experimental

Materials. Alcohol **3**, as a crude product, and sulfonate **5** were obtained in the modified procedure of a literature method.[8] 3-(4-Bromobutoxy)oxetane (**4**), bp 57—65 °C (48 Pa), was prepared in 63% yield by a phase-transfer catalytic reaction of **3** with a 3 molar amount of 1,4-dibromobutane in the presence of TBAB in hexane and 50wt% NaOH under reflux according to a method described in our previous report.[16]

Benzoic acid **8** and phenol **10** were prepared by a reaction of **4** with an equimolar amount of ethyl 4-hydroxybenzoate or 4-[(2-tetrahydropyranyl)oxy]phenol using K_2CO_3 as a base in DMF at 80 °C, followed by the hydrolysis of **7** or an acetal exchange of **9**. Similarly *m*-substituted phenol **12** was prepared by alkaline hydrolysis of the resultant ester, **11**, which was obtained by a reaction of **4** with an equimolar amount of 3-hydroxyphenyl benzoate. These products were identified with ease by IR and ^{1}H NMR spectroscopy. **7**: 65% yield, bp 80—120 °C (21 Pa); **8**: 95% yield, mp 49.2—51.5 °C (ethanol); **9**: 87% yield, mp 66.4—69.7 °C (ethanol); **10**: 96% yield, mp 66.4—69.7 °C (ethanol); **11**: 73% yield, bp 118—143 °C (21 Pa); **12**: 65% yield, mp 82.6—84.8 °C.

4-Butoxy-4′-{4-[(3-oxetanyl)oxy]butoxy}azobenzene (1a): Obtained in a 80% yield by an equimolar reaction of **3** with 4-butoxy-4′-hydroxyazobenzene using K_2CO_3 in DMF in a manner similar to that described in the previous paper:[17] IR (KBr) 3060, 1600, 1580, 1500, and 850 (1,4-phenylene), 1240 and 1060 (aromatic ether), 1110 (acyclic ether), and 965 cm^{-1} (cyclic ether); ^{1}H NMR ($CDCl_3$) δ = 0.99 (3H, t, J = 7.08 Hz, CH_3), 1.4—2.0 [total 8H: *m*, $OCH_2(CH_2)_2CH_3$ and $OCH_2(CH_2)_2CH_2O$], 3.43 (2H, t, J = 6.03 Hz, OCH_2 adjacent to the oxetane ring), 3.9—4.2 [total 4H for two triplets: δ = 4.04, J = 6.23 Hz; δ = 4.07, J = 5.86 Hz; CH_2OAr), 4.4—5.0 (total 5H, m, CH and CH_2 of the oxetane ring), and 6.9—7.9 [total 8H for two AB-*q*-like aromatic signals superimposed with each another: δ = 6.98 and 7.86, J = 8.91 Hz).

3-Oxetanyl 4-(4-Butoxyphenylazo)benzoate (6): The alcohol **3** (3.38 mmol) was stirred with 4-(4-butoxyphenylazo)benzoic acid (93.38 mmol) in THF (10 cm^3) in the presence of dicyclohexylcarbodiimide (DCC) (3.38 mmol) and 4-dimethylaminopyridine (DMAP) (1.02 mmol) at 0—5 °C for 9 h. After the ordinary post-treatment of the reaction mixture, the crude product was recrystallized from ethanol to give **6** in a 40% yield; IR (KBr) 3050, 1600, 1580, 1500, 1480, and 840, 1710, 1270, and 1230 (ester), 1250 and 1060, 1120, and 980 cm^{-1}; ^{1}H NMR ($CDCl_3$) δ = 1.00 (3H, t, J = 6.84 Hz), 1.2—2.0 (total 8H, m), 3.43 (2H, t, J = 5.54 Hz),

4.06 (2H, t, J = 6.35 Hz), 4.7—5.1 (4H, m, CH_2 of the oxetane ring), 5.70 (1H, quintet, J = 5.80 Hz, CH of the oxetane ring), and 6.9—8.2 [total 8H: AB-q-like (δ = 7.01 and 7.90, J = 8.91 Hz), $C_6H_4N_2C_6\underline{H}_4OC_4H_9$; AB-$q$-like ($\delta$ = 7.95 and 8.21, J = 8.67 Hz), $C_6\underline{H}_4N_2C_6H_4OC_4H_9$].

4-[(3-Oxetanyl)oxy]butyl 4-(4-Butoxyphenylazo)benzoate (1b): Obtained in a 63% yield by an equimolar reaction of **4** with 4-(4-butoxyphenylazo)benzoic acid in the presence of K_2CO_3 in DMF at 80 °C: IR (KBr) 3050, 1600, 1580, 1500, and 840, 1720, 1280, and 1200, 1250 and 1030, 1110, and 970 cm^{-1}; ^1H NMR ($CDCl_3$) δ = 1.00 (3H, t, J = 6.46 Hz), 1.4—2.0 (total 8H, m), 3.43 (2H, t, J = 5.74 Hz), 4.06 (2H, t, J = 6.19 Hz), 4.39 (2H, t, J = 6.35 Hz, $C\underline{H}_2OCO$), 4.4—4.9 (total 5H, m), 6.9—8.2 [total 8H: AB-q-like (δ = 7.00 and 7.94, J = 8.92 Hz), $C_6H_4N_2C_6\underline{H}_4OC_4H_9$; AB-$q$-like ($\delta$ = 7.87 and 8.18, J = 8.80 Hz), $C_6\underline{H}_4N_2C_6H_4OC_4H_9$]. Also see Fig. 1 for the ^1H NMR of **1b**.

4-(4-Butoxyphenylazo)phenyl 4-{4-[(3-Oxetanyl)oxy]butoxy}benzoate (1c-4): Obtained in a 68% yield in the same manner as the preparation of **6**: IR (KBr) 3070, 1600, 1580, 1500, and 840, 1730, 1275, and 1200, 1250 and 1060, 1100, and 970 cm^{-1}; ^1H NMR ($CDCl_3$) δ = 1.00 (3H, t, J = 6.72 Hz), 1.4—2.0 (total 8H, m), 3.44 (2H, t, J = 5.86 Hz), 3.9—4.2 (total 4H for two triplets: δ = 4.05, J = 6.10 Hz; t, δ = 4.09, J = 5.86 Hz), 4.4—4.9 (total 5H, m), and 6.9—8.2 (total 12H for three AB-q-like patterns: δ = 6.97 and 8.17, J = 8.92 Hz; δ = 7.00 and 7.91, J = 8.91 Hz; δ = 7.34 and 7.96, J = 8.79 Hz).

4-[4-(Octyloxy)phenylazo]phenyl 4-{4-[(3-Oxetanyl)oxy]butoxy}benzoate (1c-8): Obtained in a 78% yield in the above-mentioned procedure: IR (KBr) 3060, 1600, 1580, 1510, 1500, 1470, and 840, 1730, 1270, and 1200, 1260 and 1060, 1100, and 980 cm^{-1}; ^1H NMR ($CDCl_3$) δ = 0.89 (3H, t, J = 6.72 Hz), 1.2—1.6 [10H, m, $OCH_2CH_2(C\underline{H}_2)_5CH_3$], 1.7—2.0 (total 6H: m, $OCH_2(C\underline{H}_2)_2CH_2O$ and $OCH_2C\underline{H}_2C_6H_{13}$), 3.44 (2H, t, J=5.86 Hz), 3.9—4.2 (total 4H for two triplets: δ = 4.04, J = 6.34 Hz; δ = 4.09, J = 5.86 Hz), 4.4—4.9 (total 5H, m), and 6.9—8.2 (total 12H for three AB-q-like patterns: δ = 6.97 and 8.17, J = 8.92 Hz; δ = 7.00 and 7.91, J = 9.04 Hz; δ = 7.34 and 7.96, J = 8.79 Hz).

4-[4-(Decyloxy)phenylazo]phenyl 4-{4-[(3-Oxetanyl)oxy]butoxy}benzoate (1c-10): Obtained in a 85% yield in the above-mentioned procedure: IR (KBr) 3060, 1600, 1580, 1510, 1500, and 840, 1720, 1290, and 1200, 1250 and 1080, 1100, and 970 cm^{-1}; ^1H NMR ($CDCl_3$) δ = 0.88 (3H, t, J = 6.59 Hz), 1.2—1.6 (total 14H, m), 1.7—2.0 (total 6H, m), 3.44 (2H, t, J = 5.86 Hz), 3.9—4.2 [total 4H for two triplets: δ = 4.04, J = 6.34 Hz; δ = 4.09, J = 5.86 Hz), 4.4—4.9 (total 5H, m), and 6.9—8.2 (total 12H for three AB-q-like patterns: δ = 6.97 and 8.16, J = 9.04 Hz; δ = 7.00 and 7.91, J = 9.04 Hz; δ = 7.33 and 7.96, J = 8.90 Hz).

4-{4-[(3-Oxetanyl)oxy]butoxy}phenyl 4-(4-Butoxyphenylazo)benzoate (1d): Obtained in a 31% yield in the above-mentioned procedure: IR (KBr) 3060, 1600, 1580, 1510, and 840, 1730, 1280, and 1200, 1250 and 1080, 1110, and 970 cm^{-1}; ^1H NMR ($CDCl_3$) δ = 1.00 (3H, t, J = 6.59 Hz), 1.6—2.0 (total 8H, m), 3.43 (2H, t, J = 5.86 Hz), 3.9—4.2 [total 4H for two triplets: δ = 4.01, J = 5.86 Hz; δ = 4.07, J = 6.11 Hz), 4.4—4.9 (total 5H, m), and 6.8—8.4 [total 12H for three AB-q-like patterns: δ = 6.90 and 7.17, J = 9.16 Hz; δ = 7.03 and 7.95, J = 8.79 Hz; δ = 7.95 and 8.32, J = 8.43 Hz).

3-{4-[(3-Oxetanyl)oxy]butoxy}phenyl 4-(4-Butoxyphenylazo)benzoate (*m*-1d): Obtained in a 45% yield in the above-mentioned procedure: IR (KBr) 3060, 1600, 1580, 1500, 1480, 780, and 690 (1,3-phenylene), 1730, 1270, and 1190, 1260 and 1070, 1100, and 960 cm^{-1}; ^1H NMR ($CDCl_3$) δ = 1.00 (3H, t, J = 6.46 Hz), 1.6—2.0 (total 8H, m), 3.42 (2H, t, J = 6.10 Hz), 3.9—4.2 (total 4H for two triplets: δ = 4.01, J = 5.85 Hz; δ = 4.07, J = 6.11 Hz), 4.4—4.9 (total 5H, m), and 6.7—8.4 [total 12H: m (δ = 6.7—6.9), aromatic protons ortho and para to the acyloxy of OC_6H_4OCO; AB-q-like (δ = 7.02 and 7.96, J = 8.91 Hz), $C_6H_4N_2C_6\underline{H}_4OC_4H_9$; m (δ = 7.2—7.4), aromatic proton meta to the acyloxy of OC_6H_4OCO; AB-q-like (δ = 7.96 and 8.33, J = 8.67 Hz), $C_6\underline{H}_4N_2C_6H_4OC_4H_9$].

The elemental analysis data of the monomers were summarized in Table 2.

Polyoxetanes: These polymers were prepared in the manner described in our previous report.[1,2] Their IR (KBr) and ^1H NMR ($CDCl_3$) data are as follows.

Poly(1a): IR 1250 (aromatic ether), 1150 (acyclic ether), and 840 cm^{-1} (1,4-phenylene); ^1H NMR δ = 0.95 (3H, t, CH_3), 1.2—2.0 (8H, m, $OCH_2(CH_2)_2CH_2O$ and $OCH_2(CH_2)_2CH_3$), 3.3—3.7 [7H, m, CH and CH_2 of the polymer backbone and $OC\underline{H}_2(CH_2)_3OAr$], 3.8—4.1 (4H, m, CH_2OAr), 6.7—7.0 (4H, aromatic protons ortho to the tail and the spacer), and 7.6—7.9 (4H, aromatic protons ortho to the azo).

Poly(1b): IR 1715 and 1270 (ester), 1260, 1110, and 840 cm^{-1}; ^1H NMR δ = 0.96 (3H, t), 1.3—2.0 (8H, m), 3.3—3.7 [7H, m, CH and CH_2 of the polymer backbone and $OC\underline{H}_2(CH_2)_3OCO$], 3.97 [2H, t, $O(CH_2)_3C\underline{H}_2OCO$], 4.30 (2H, t, CH_2OAr), 6.8—7.1 (2H, aromatic protons ortho to the butoxy), 7.7—8.0 (4H, aromatic protons ortho to the azo), and 8.0—8.2 (2H, aromatic protons ortho to the acyl).

Poly(1c-4): IR 1375, 1270(sh), and 1200, 1250 and 1070, 1170 and 1150, and 840 cm^{-1}; ^1H NMR δ = 0.97 (3H, t), 1.2—2.0 (8H, m), 3.3—3.7 (7H, m), 3.7—4.1 (4H, m), 6.8—7.0 (4H, aromatic protons ortho to the tail and the spacer), 7.1—7.4 (2H, aromatic protons ortho to the acyloxy), 7.7—8.0 (4H), and 8.0—8.2 (2H).

Poly(1c-8): IR 1730, 1280(sh), and 1200, 1250 and 1070, 1170 and 1150, and 840 cm^{-1}; ^1H NMR δ = 0.89 (3H, t), 1.2—1.6 [10H, m, $OCH_2CH_2(C\underline{H}_2)_5CH_3$], 1.6—2.0 [6H, m, $OCH_2(C\underline{H}_2)_2CH_2O$ and $OCH_2C\underline{H}_2C_6H_{13}$], 3.4—3.8 (7H, m), 3.8—4.2 (4H, m), 6.8—7.0 (4H), 7.1—7.4 (2H), 7.7—8.0 (4H), and 8.0—8.2 (2H).

Poly(1c-10): IR 1730, 1270(sh), and 1200, 1250 and 1070, 1170 and 1150, and 840 cm^{-1}; ^1H NMR δ = 0.88 (3H, t), 1.2—1.6 (16H, m), 1.6—2.0 (6H, m), 3.4—3.8 (7H, m), 3.8—4.2 (4H, m), 6.8—7.0 (4H), 7.1—7.4 (2H), 7.7—8.0 (4H), and 8.0—8.2 (2H).

Poly(1d): IR 1730, 1275(sh), and 1950, 1250 and 1070, 1140 and 1100, and 860 and 840 cm^{-1}; ^1H NMR δ = 0.99 (3H, t), 1.3—2.0 (8H, m), 3.3—3.7 (7H, m), 3.8—4.1 (4H, t), 6.7—7.2 (4H), 7.7—8.0 (4H), and 8.1—8.4 (2H).

Poly(*m*-1d): IR 1730, 1260 and 1060, 1260 and 1060, 1130, and 855 and 825 cm^{-1} (1,3-phenylene); ^1H NMR δ = 0.97 (3H, t), 1.3—2.0 (8H, m), 3.3—3.7 (7H, m), 3.8—4.1 (4H, t), 6.4—6.8 (3H, aromatic protons ortho and para to the spacer), 6.8—7.0 (2H, aromatic protons ortho to the tail), 7.0—7.3 (1H, aromatic protons meta to the spacer), 7.7—8.0 (4H, aromatic protons ortho to the azo), and 8.1—8.3 (2H, aromatic protons ortho to the acyl).

The elemental analysis data of the polymers were also shown in Table 2.

Measurement. IR and ^1H NMR spectroscopy, GPC, DSC, and X-ray diffractmetry were performed in the manner described in our previous reports.[1,17]

References

1) H. Ogawa, T. Hosomi, T. Kosaka, S. Kanoh, A. Ueyama, and M. Motoi, *Bull. Chem. Soc. Jpn.*, **70**, 175 (1997).

2) H. Ogawa, S. Kanoh, and M. Motoi, *Bull. Chem. Soc. Jpn.*, **70**, 1649 (1997).
3) Y. Kawakami, K. Takahashi, and H. Hibino, *Macromolecules*, **24**, 4531 (1991).
4) Y. Kawakami, M. Suzuki, Y. Kato, and A. Mori, *Polym. J.*, **28**, 845 (1996).
5) Y.-H. Lu and C.-S. Hsu, *Macromolecules*, **66**, 1673 (1995).
6) Y. Kawakami, K. Takahashi, S. Nishiguchi, and K. Toida, *Polym. Int.*, **31**, 35 (1993).
7) H. Ogawa, J. Yamamoto, A. Ueyama, S. Kanoh, and M. Motoi, "SPSJ 43rd Symposium on Macromolecules," Fukuoka, Oct. 1994, Japan, Polym. Preprints, Abstr., No. 13L12.
8) K. Baum, P. T. Berkowitz, V. Grakauskas, and G. Archibald, *J. Org. Chem.*, **48**, 2953 (1983).
9) P. Dreyfuss and M. P. Dreyfuss, *Polym. J.*, **8**, 81 (1976).
10) M. Bucquoye and E. J. Goethals, *Makromol. Chem.*, **179**, 1681 (1978).
11) M. R. Bucquoye and E. J. Goethals, *Polym. Bull.*, **22**, 707 (1980).
12) E. J. Corey and N. Raju, *Tetrahedron Lett.*, **24**, 5571 (1983).
13) M. Motoi, S. Sekizawa, K. Asakura, and S. Kanoh, *Polym. J.*, **25**, 1283 (1993).
14) L. March, "Advanced Organic Chemistry," 4th ed, J. Wiley & Sons, New York (1992), p. 152.
15) E. Pérez, A. Bello, and J. M. Pereña, *Polym. Bull.*, **20**, 291 (1988).
16) M. Motoi, S. Nagahara, M. Yokohama, E. Saito, O. Nishimura, S. Kanoh, and H. Suda, *Bull. Chem. Soc. Jpn.*, **62**, 1572 (1989).
17) M. Motoi, K. Noguchi, A. Arano, S. Kanoh, and A. Ueyama, *Bull. Chem. Soc. Jpn.*, **66**, 1778 (1993).